

**ApoFnr binds as a monomer to promoters regulating the expression of
enterotoxin genes of *Bacillus cereus***

Running title: Active aerobic apoFnr is monomeric

Julia Esbelin¹, Yves Jouanneau², Jean Armengaud³ and Catherine Duport^{1*}

¹Université d'Avignon, UMR A408, Sécurité et Qualité des Produits d'Origine Végétale;
INRA, Avignon, F-84914, France.

² Laboratoire de Chimie et Biologie des Métaux, UMR 5249, CEA-Grenoble cedex 09, F-
38054, France.

³ Laboratoire de Biochimie des Systèmes Perturbés, CEA-Marcoule, SBTN, BP17171,
Bagnols-sur-Cèze cedex, F-30207, France.

* Corresponding author. Mailing address: UMR A408, INRA, site Agroparc, 84914 Avignon
cedex 9, France.

Phone: +33 4 32 72 25 07. Fax: +33 4 32 72 24 92. E-mail: catherine.duport@univ-avignon.fr

22 Abstract

23 *Bacillus cereus* Fnr is a member of the Crp/Fnr (cAMP-binding protein/fumarate
24 nitrate reduction regulatory protein) family of helix-turn-helix transcriptional regulators. It is
25 essential for the expression of *hbl* and *nhe* enterotoxin genes independently of the oxygen
26 tension in the environment. We studied aerobic Fnr binding to target sites in promoters
27 regulating the expression of enterotoxin genes. *B. cereus* Fnr was overexpressed and purified
28 as either a C-terminal His-tagged (Fnr_{His}) or an N-terminal Strep-tagged (StrepFnr) fusion
29 protein. Both recombinant Fnrs were produced as apoforms (clusterless) and occurred as
30 mixtures of monomer and oligomers in solution. However, apoFnr_{His} was mainly monomeric,
31 while apoStrepFnr was mainly oligomeric, suggesting that the His-tagged C-terminal extremity
32 may interfere with oligomerization. The oligomeric state of apoStrepFnr was dithiothreitol-
33 sensitive, underlining the importance of a disulphide bridge for apoFnr oligomerization.
34 Electrophoretic mobility shift assays showed that monomeric, but not oligomeric apoFnr,
35 bound to specific sequences located in the promoter regions of the enterotoxin regulators *fnr*,
36 *resDE* and *plcR* and the structural genes *hbl* and *nhe*. The question of whether apoFnr binding
37 is regulated *in vivo* by redox-dependent oligomerization is discussed.

38

39 INTRODUCTION

40 The facultative anaerobic, spore-forming *Bacillus cereus* has gained notoriety as an
41 opportunistic human pathogen that can cause a wide range of diseases from periodontitis and
42 endophthalmitis to meningitis in immunocompromised patients.. However, most of the
43 reported illnesses involving *B. cereus* are food-borne intoxications, classified as emetic and
44 diarrheal syndromes (17, 30). Diarrheal syndrome may result from the production in the
45 human host's small intestine of various extracellular factors including hemolysin BL (Hbl),
46 non-haemolytic enterotoxin (Nhe) and cytotoxin CytK (17, 26). The genes encoding these
47 potential virulence factors belong to the PlcR regulon (1, 7, 20, 31).

48 *B. cereus* will grow efficiently by anaerobic glucose fermentation in amino acid-rich
49 media supplemented with glucose as the major source of carbon and energy (3, 21, 29, 33,
50 34). The ability of *B. cereus* to grow well under these conditions is controlled by both the
51 two-component system ResDE (4) and the redox regulator Fnr (33, 34). Unlike ResDE, *B.*
52 *cereus* Fnr has been shown to be essential for fermentative growth and for enterotoxin
53 synthesis under both anaerobiosis and aerobiosis (33, 34). Fnr protein is a member of the
54 large Crp/Fnr superfamily of transcription factors that coordinate physiological changes in
55 response to a variety of metabolic and environmental stimuli (16). Members of the family are
56 predicted to be structurally related to the catabolite gene activator protein of *Escherichia coli*,
57 Crp (also known as the cAMP receptor protein) (10). Like all the members of the Crp/Fnr
58 family, *B. cereus* Fnr contains an N-terminal region made up of antiparallel β -strands able to
59 accommodate a nucleotide, and a C-terminal helix-turn-helix (HTH) structural motif. In
60 addition, it contains a C-terminal extension with four cysteine residues considered, in
61 *B. subtilis*, to coordinate a $[4\text{Fe-4S}]^{+2}$ centre that serves as a redox sensor (27). The *B. subtilis*
62 Fnr forms a stable dimer that is independent of both the oxygen tension in the environment

and FeS cluster formation. However, the presence of an intact $[4\text{Fe-4S}]^{+2}$ cluster is required for it to bind to a specific DNA-binding site and for subsequent transcriptional activation (27).

Structurally, the predicted Fnr of *B. cereus* resembles the *B. subtilis* Fnr (27). Therefore, the FeS cluster could also be a key component required for the DNA binding activity of *B. cereus* Fnr under anaerobiosis. However, our previous results suggested that unlike *B. subtilis* Fnr, *B. cereus* Fnr may also exist in an active state under aerobiosis and thus conserve some site-specific DNA binding properties. To address this specificity further and elucidate the mechanism by which Fnr regulates enterotoxin gene expression in aerobically growing *B. cereus* cells, we characterized the DNA-binding activities of purified aerobic Fnr. To this end, we overproduced full-length Fnr in *Escherichia coli* with two different tags. We showed that both recombinant Fnrs were produced in apo forms (devoid of FeS cluster) under oxic conditions. Recombinant Fnr containing a C-terminal polyhistidine tagged sequence was shown to be mainly monomeric in solution, while N-terminally Strep-tagged Fnr occurred mainly as oligomers. Only the monomeric forms of both recombinant apoFnrs were found to bind to the promoter regions of *fnr* itself, the pleiotropic regulators *resDE* and *plcR* and the structural enterotoxin genes *hbl* and *nhe*. Finally, our results pointed to some new unusual properties of Fnr that may have physiological relevance in the redox regulation of enterotoxin expression, enterotoxin expression being both directly and indirectly (via ResD and PlcR) regulated by apoFnr under aerobiosis.

MATERIALS AND METHODS

Bacterial strains and growth conditions. *Escherichia coli* strain TOP 10 (Invitrogen) [F^- *mcrA* Δ (*mrr-hsdRMS-mcrBC*) Φ 80*lacZ* Δ *M15* Δ *lacX74* *deoR* *recA1* *araD139* Δ (*ara-leu*)-7697 *galU* *galK* *rpsL* (Str^r) *endA1* *nupG*] was used as the general cloning host, and strain BL21 CodonPlus(DE3)-RIL (Stratagene) [F^- *ompT* *hsdS*(r_B^- m_B) *dcm*⁺ *Tet*^r *gal* λ (DE3) *endA* *Hte*

[*argU ileY leuW* Cam^r] was used to overexpress *fnr*. Both *E. coli* strains were routinely grown in Luria broth with vigorous agitation at 37°C. *B. cereus* F4430/73 wild-type (32) and *fnr* mutant (34) were grown as previously described.

General molecular methods. Restriction endonuclease and T4 DNA ligase were obtained from Promega and used in accordance with the manufacturer's instructions. Genomic DNA of *B. cereus* was purified as described by Guinebretiere and Nguyen-The (11). Plasmid DNA was purified using anion-exchange columns (Promega). PCR amplification of DNA was carried out with *Taq* polymerase using the manufacturer's specifications (Roche Molecular Biochemicals) for reaction conditions. The 5' end of the *resDE* mRNA was mapped from a 5' RACE PCR product obtained with the 3'/5' RACE kit (Rapid amplification of cDNA ends, Roche Molecular Biochemicals). For this purpose, we used total RNA extracted from *B. cereus* F4430/73 cells harvested at μ_{\max} , *i.e.* the maximal expression of the *resDE* operon. Briefly, the first-strand cDNA was synthesized from total RNA with *fnr*-specific primer SP1 (5'-GCCTGGTAAAGATGGCATTG-3'), avian myeloblastosis virus reverse transcriptase, and the deoxynucleotide mixture of the 3'/5' RACE kit as recommended by the manufacturer. After purification and dA tailing of the cDNA, a PCR with the (dT)-anchor oligonucleotide primer and the specific *fnr* SP2 primer (5'-GATGATGAGGATCGTATTVGTCG-3') followed by a nested PCR with SP3 primer (5'-GAGAGTGCGCAGCGGGTAGAG-3') yielded a PCR product of 190 bp, as revealed by 2% agarose gel electrophoresis. This PCR product was purified and sequenced.

Cloning and overexpression of recombinant Fnr. The coding sequence for *B. cereus fnr* was PCR-amplified from F4430/73 genomic DNA using either primers PET101F (5'-CACCGTGGCAAACAGTATGACATTATCT-3') and PET101R (5'-ATCAATGCTACAAA

113 CAGAAGC-3') or primers PET52F (5'-**CCCGGG**ATGACATTATCTCAAGATTAAAAAG
114 AA-3'; *Sma*I restriction site in bold type) and PET52R (5'-
115 **GAGCTC**CTAATCAATGCTACAAACAGAAGCA-3'; *Sac*I restriction site in bold type).
116 The amplicons were cloned as blunt-end PCR product into pET101/D-TOPO (Invitrogen) and
117 as a *Sma*I-*Sac*I fragment into the corresponding sites of pET-52b(+) (Novagen), yielding
118 pET101*fnr* and pET52*fnr*, respectively. *B. cereus* Fnr was produced as a C-terminal fusion
119 with a His-tag using pET101*fnr* (Fnr_{His}) and as an N-terminal fusion with a Strep-tag using
120 pET52*fnr* (StrepFnr) in *E. coli* BL21 CodonPlus(DE3)-RIL (Stratagene). Recombinant cells
121 were grown at 37°C in Luria broth with 100 µg ml⁻¹ ampicillin. When OD₆₀₀ reached ~1.0,
122 protein production was triggered by adding isopropyl-β-D-thiogalactopyranoside (IPTG) with
123 a final concentration of 0.2 mM (pET101*fnr*) or 0.4 mM (pET52*fnr*). Cells were further
124 grown for 16 h at 20 °C.

125
126 **Purification of Fnr_{His}** Cells from a 4.8 L culture were harvested by centrifugation (10,000g,
127 15 min), resuspended in buffer A (50 mM sodium phosphate buffer [pH 7.0], 300 mM NaCl,) and
128 incubated with 0.5 mg/ml lysosyme for 30 min under gentle agitation. Cells were lysed
129 by sonication for 3 min at 80% of maximum amplitude using a Vibra cell ultrasonifier (Fisher
130 Bioblock Scientific). Cell debris were removed by centrifugation at 20,000g for 20 min. The
131 supernatant was run through a 5 ml Co²⁺ IMAC column (Clontech) equilibrated with buffer
132 A. The column was washed with 50 ml of buffer A and then with 25 ml of buffer A
133 containing 10 mM imidazole, and the protein was eluted with 5 ml of buffer A containing 150
134 mM imidazole. The eluted fraction was desalted on a Sephadex G25 column (Amersham
135 Pharmacia Biotech) and concentrated using Nanosep 30 kDa molecular-weight-cutoff devices
136 (Omega disc membrane, Pall Filtron). Concentrated samples were run through a 104 ml
137 Superdex SD200 column (Amersham Biosciences) equilibrated with buffer B (100 mM Tris-
138 HCl [pH 8], 150 mM NaCl, 1 mM DTT). Protein was stored as pellets in liquid nitrogen.

140 **Purification of $\text{Fnr}_{\text{strep}}$.** Cells from a 6 L culture were harvested by centrifugation at 10,000g
141 for 15 min, resuspended in 120 ml of buffer C (25 mM Tris-HCl [pH 8], 1 mM DTT) and
142 incubated with 0.2 mg.ml⁻¹ of lysozyme and 0.5 mM EDTA for 10 min at 30 °C. Cells were
143 lysed by sonication as described above for the purification of Fnr_{His} . Cell debris were
144 removed by centrifugation at 43,000g for 1 h and the resulting supernatant was run through a
145 30 ml DEAE-cellulose column (DE52; Whatman) equilibrated with buffer C. The column
146 was then washed with the same buffer. Non-retained fractions were adjusted to pH 7 with 1M
147 KH_2PO_4 and run through a 30 ml hydroxyapatite agarose column (HA Ultrogel; Pall
148 Corporation) equilibrated with buffer D (50 mM KH_2PO_4 [pH 7], 1 mM DTT). The column
149 was developed with a linear gradient from 50 to 200 mM KH_2PO_4 at a flow rate of 2 ml/min.
150 Fractions containing recombinant Fnr were pooled and concentrated to 48 mg. ml⁻¹ by
151 ultrafiltration through an Omega disc membrane (30 kDa cut-off, Ø 43 mm, Pall Filtron). A
152 polishing step was then carried out with gel filtration on a 104 ml Superdex SD200 column
153 (Amersham Biosciences) equilibrated with buffer D containing 150 mM NaCl. The purified
154 protein was stored as pellets in liquid nitrogen.

155 **Protein biochemical analyses.** Protein concentrations were determined by either a BCA
156 (bicinchoninic acid) assay according to the manufacturer's instructions (Interchim) or a Biuret
157 method insensitive to thiols (22). Bovine serum albumin (BSA) was used as standard.
158 Overproduction of Fnr in induced cultures and its purification were monitored by SDS-
159 PAGE. The Laemmli method was used for SDS-PAGE (18). Proteins were stained with
160 Coomassie brilliant blue. Reducing agent β -mercaptoethanol was omitted when analysing the
161 disulphide form of apoFnr. The molecular mass of apoFnr was accurately measured with an
162 Esquire 3000plus ion trap mass spectrometer equipped with a nanoelectrospray on-line ion

source (Bruker Daltonics) essentially as described in (6). Before mass measurement, purified apoFnr was desalted with a ZipTip_{C18} (Millipore), and diluted in acetonitrile/formic acid (50%/1%, v/v).

Dynamic Light Scattering (DLS). The quaternary structure of purified apoFnr in solution was measured by DLS. Samples were centrifuged and run through a 24 mL Superdex 200 column (HR10/30) equilibrated and run at a flow rate of 0.5 ml/min with 50 mM TRIS/HCl pH 8.3 containing 120 mM NaCl and 0.05% NaN₃ filtered at 0.1 μm. The column was operated with an Agilent 1100 Series reverse-phase high-performance liquid chromatography (HPLC) system equipped with G1322A degasser, G1311A quaternary pump, and G1313A autosampler. The elution profile was monitored with a G1315B diode array detector (Agilent), a miniDawn Tristar Multi-angle laser Static Light Scattering detector (three angles, 45°, 90° and 135°) coupled to a DynaPro Titan Light Scattering Instrument (Wyatt technology) placed at 90° and an Optilab rEX differential refractometer (Wyatt technology). The 90° MALS detector was calibrated with pure toluene, and BSA was then used to normalize the other detector (45° and 135°) in the corresponding buffer.

Chemical cross-linking of Fnr_{His}. Fnr_{His} in 10 mM 3-(N-morpholino) propanesulfonic acid (MOPS) buffer (pH 7.75) was treated with protein crosslinking agents, *N*-hydroxysulfosuccinimide (5 mM) and 1-ethyl-3-[3-dimethylaminopropyl]carbodiimide hydrochloride (EDC;12.5 mM). The reaction mixture contained protein at a concentration of 5 μM in a total reaction volume of 20 μl. The reaction was allowed to proceed for 30 min at room temperature and stopped by adding 25 mM β-mercaptoethanol. The products were analyzed by 12% non-denaturing SDS-PAGE and detected by Western blot using an anti-His antibody.

188

189 **ApoFnr antiserum preparation.** Polyclonal antibodies against apoFnr were generated in-
190 house. Rabbits were immunized with a total of 2 mg of purified Fnr_{His}, administered in four
191 equal doses over a 90-day period, and bled on Day 120. Antisera specificities were checked
192 by Western blot.

193

194 **Western blot analysis.** *B. cereus* protein extracts were prepared as follows: cells were
195 harvested by centrifugation, resuspended in buffer containing 8 M urea, 4% (w/v) CHAPS
196 ([3-[(3-cholamidopropyl)-dimethylammonio]propanesulfonate]), and mechanically disrupted
197 using a FastPrep instrument (FP120, Bio101, Thermo Electron Corporation). Cell debris were
198 removed by centrifugation (3,500g, 10 min, 4 °C). Proteins were then filtered and resolved by
199 SDS-PAGE under non-reducing conditions (18). Resolved proteins were transferred to
200 nitrocellulose membranes (Amersham Bioscience) in a Biorad liquid/liquid transfer unit. As
201 appropriate, ApoFnr was detected with either anti-His antibodies (Fnr_{His}) or anti-Strep
202 antibodies (Strep^{Fnr}), or with 1:2000 dilution of polyclonal rabbit serum. The blotted
203 membranes were developed with a 1:2000 dilution of peroxidase-conjugated goat anti-rabbit
204 IgG (Sigma) and an enhanced chemiluminescence substrate (Immobilon Western, Millipore).

205

206 **Electrophoretic Mobility Shift Assay (EMSA).** The 5'untranslated regions (UTR) of *fnr*,
207 *resDE*, *plcR*, *hbl*, and *nhe* were PCR amplified with the following primer pairs: FnrF (5'-
208 CGAACACTTCAGCAGGCATA-3') and FnrR (5'-AATGTCATACTGTTTGCCAC-3'),
209 ResDF (5'-TGGGATCCCAAAGAGGTTTG-3') and ResDR (5'-CGATCC
210 TCATCATCTACAAT-3'), PlcRF (5'-TATGTTTGTGCAAGGCGAAC-3') and PlcRR (5'-
211 CCTAATTTTCTGCGTGCAT-3'), Hbl1F (5'-GGTAAGCAAGTGGGTGAAGC-3') and
212 Hbl1R (5'-AATCGCAAATGCAGAGCACAA-3'), Hbl2F (5'-

TTAACTTAATTCATATACTT-3') and Hbl2R (5'-TACGCATTAAAAATTTAAT-3'),
 NheF (5'-TGTTATTACGACAGTTCCAT-3') and NheR (5'-
 CTGTAACCAATAACCCTGTG-3'), respectively. The forward primers were 5' end labelled
 with T4 polynucleotide kinase (Promega) and [γ - 32 P]ATP (Amersham Biosciences). The 5'-
 32 P labelled amplicons were purified using High Pure PCR Product Purification columns
 (Roche). EMSAs were performed by incubating labelled DNA fragments (1000 cpm per
 reaction) with the specified amount of purified Fnr in 50 mM Tris-HCl [pH 7.5] buffer
 containing 50 mM KCl, 0.1 mM EDTA, 10% glycerol, 4 mM dithiothreitol, 4 mM MgCl₂, 0.5
 µg of bovine serum albumin and 1 µg of poly(dI-dC)/ml in a final volume of 10 µl. Binding
 reactions were incubated for 30 min at 37°C and then loaded onto a 4% or 6% non-denaturing
 polyacrylamide gel run with Tris-borate-EDTA buffer at 4 °C and 200 V. Labelled products
 were quantified using a Molecular Dynamics PhosphoImager.

RESULTS

Overexpression and purification of two recombinant Fnr proteins

From the sequence alignment of 13 *B. cereus* Fnr homologues (see Fig. S1 in
 supplementary data), two possible alternative translation initiation starts could be identified
 for *B. cereus* F4430/73: GTG as previously defined (34) or ATG, 12 nucleotides further on.
 Taking into account this information, two procedures were developed for the aerobic
 production of *B. cereus* F4430/73 Fnr in *E. coli* cells: (i) expression of a His-tag fusion
 protein from pET101/D-TOPO to release a Fnr variant (Fnr_{His}) that begins with the valine
 encoded by the predicted start codon of *B. cereus* (34) and contains 30 additional amino acids
 at the C-terminal end, and (ii) expression of a Strep-Tag fusion from pET-52b(+) to release an
 Fnr variant (StrepFnr) that contains 22 additional amino acids at the N-terminal end. In the

latter variant, the first amino acid of the native Fnr is the methionine located 4 amino acids after the valine encoded by the predicted start codon (see Fig. S1 in supplementary data). The Fnr_{His} protein was purified using cobalt affinity chromatography. Because preliminary tests indicated that _{Strep}Fnr bound very weakly to Strep-tactin sepharose (IBA), the tagged protein was purified by means of three successive chromatography runs not based on the tag affinity. On SDS-PAGE, purified Fnr_{His} (29 kDa) and _{Strep}Fnr (28 kDa) exhibited the expected molecular masses (See Fig. S2 in supplementary data). The exact average molecular mass of _{Strep}Fnr determined by mass spectrometry was $27,913 \pm 2$ Da. This value corresponds almost perfectly (75 ppm deviation) to the expected polypeptide sequence, except that the initial formyl-methionine is cleaved (theoretical value: 27,911 Da). This maturation probably also occurs with the Fnr_{His} protein.

UV-visible absorption spectrum of both aerobic recombinant forms of Fnr showed a single peak at 280 nm (data not shown), suggesting that there is no absorbing prosthetic group (14). This indicates that both recombinant Fnr forms were purified as apoproteins under aerobiosis.

Oligomeric state of both recombinant apoFnr proteins.

DLS was used to examine the oligomeric state of the two recombinant forms of apoFnr. DLS reveals the homogeneity and oligomeric state of proteins when resolved by gel filtration based on the scattering of visible light by particles (5). The oligomerization states of Fnr_{His} and _{Strep}Fnr were analyzed using a DynaPro Titan DLS instrument and attendant software ASTRA. Figure 1 shows the elution profile obtained for both proteins and the molecular mass estimates derived from the light scattering signal. Besides a peak of aggregates at 16 min, Fnr_{His} was resolved into four elution peaks at 22.0 (A1), 26.6 (A2), 28.8 (A3) and 30.7 (A4) min elution time as detected on the UV trace (Fig. 1A). The molar mass

across peak A1 could not be determined because of a polydisperse distribution (the molecular mass varied from 170 to 400 kDa). This strongly suggests that this peak contained aggregates that interacted with the column, but their proportion was low, as the DLS signal was very weak. In contrast, the distribution of molar masses across peaks A2, A3 and A4 was constant, indicating a monodisperse distribution (*i.e.* a homogeneous molecule) for each peak with molecular masses of 98 (A2), 60 (A3) and 30 (A4) kDa (+/- 3%), respectively. This indicates that Fnr_{His} occurs mainly as a mixture of trimer, dimer and monomer in solution. Considering the relative mass ratio that can be estimated from the UV trace, the predominant form was the monomer (70%). The light scattering trace obtained with _{Strep}Fnr showed the presence of aggregates (peak B1) and three peaks with molecular masses of 157 (B2), 106 (B3) and 54 (B4) kDa (+/- 3%), respectively (Fig. 1B). These peaks unambiguously correspond to the hexameric, tetrameric and dimeric forms of _{Strep}Fnr, respectively. In this case, the dimeric form (33%) formed the largest population. The same DLS experiment was repeated in reducing conditions with 10 mM DTT in the elution buffer. Complete disappearance of the hexameric form and almost complete disappearance of the tetrameric form (C1) were observed (Fig. 1C). The dimeric form (C2) was thus predominant (89%). Hence the addition of reductant affected the oligomerization state of _{Strep}Fnr in solution. Intermolecular disulphide bridges are involved in the formation of the highest oligomeric forms. In addition, the absence of monomers in reducing conditions suggests that the dimers observed were either non-covalently linked structures or DTT-resistant covalently linked structures.

When purified _{Strep}Fnr underwent SDS-PAGE in non-reducing conditions (no DTT or β -ME) a multiple-band pattern was observed, revealing the presence of a mixed population of monomer, dimer and higher oligomeric forms in relative ratios compatible with those found in a DLS experiment (Fig. 2A). In reducing conditions (with DTT), the two major species were the monomeric and the dimeric forms. Increasing the concentration of DTT from 10 mM to

200 mM caused the total reduction of dimeric species to monomeric forms. These data indicate that most of the protein was reticulated through disulphide bridges, but a significant amount of dimeric Fnr_{His} could either not be completely reduced by DTT or remained particularly stable in the electrophoresis conditions used. In contrast, only a very small fraction of Fnr_{His} was found to remain dimeric after 10 mM DTT treatment (Fig. 2B). This suggests that the oligomeric Fnr_{His} population detected by DLS contained mainly non-covalently linked structures. To investigate the ability of monomeric Fnr_{His} to form covalently linked structures, a fraction of the purified protein was treated with either the chemical cross-linker EDC or with the divalent thiol-reactive agent diamide. The first cross-linker modifies an ionic interaction into a covalent link, while the latter mimics disulphide bridge formation. Figure 2 shows the reaction products analyzed by SDS-PAGE. Formation of oligomers from monomer could be evidenced using both EDC (Panel C) and diamide (Panel D). Homodimers and homotrimers were the major products. As expected when using crosslinkers, these entities migrated at relative molecular weights slightly lower than the exact weights because of their more rigid structures. Surprisingly, the band corresponding to apoFnr monomer appeared as a discrete doublet after treatment with diamide, reflecting a possible induced conformational change trapped by intrapolypeptide crosslinks (Fig. 2D). In conclusion, Fnr_{His} monomers were able to self-associate and form higher-order covalently linked structures in the presence of cross-linkers. This suggests that unlike Fnr_{His} , Fnr_{His} does not tend to form covalently linked homodimers or, more specifically, intermolecular disulphide bridges.

Detection of endogeneous apoFnr in *B. cereus* F4430/73 cells.

To determine whether the formation of disulphide-linked homodimers might be of physiological relevance, we tested the presence of various forms of endogenous apoFnr in aerobically grown *B. cereus* cells (4). Figure 3 shows the Western blot detection performed

with apoFnr antiserum following SDS-PAGE under non-reducing conditions. The antiserum reacted with two bands of the sizes expected for the monomeric (~30 kDa) and dimeric forms (~60 kDa) of apoFnr in wild-type cells, but not in *fnr* mutant cells. Two other protein bands of 40 and 80 kDa cross-reacted with apoFnr antiserum in wild-type cells (Fig. 3, lane 3). As these bands were also observed in the *fnr* mutant cells (Fig. 3, lane 2), they were not related to Fnr. Finally, these results indicated that the apoFnr antiserum can be used efficiently for the detection of endogenous apoFnr in *B. cereus* F4430/73 cells and, more importantly, that some dimeric apoFnr could be disulphide-linked in *B. cereus*

Binding of apoFnr to the 5' untranslated regions of *fnr*, *resDE*, *plcR*, *hbl* and *nhe*

The amino acid residues forming the REX₃R motif within the HTH DNA-binding domain of Crp regulatory proteins are strictly conserved in the potential DNA-binding domain of *B. cereus* F4430/73 Fnr as in its homologues found in strains belonging to *B. cereus* group (12). Accordingly, Fnr of *B. cereus* F4430/73 was assumed to bind to DNA motifs similar to the TGTGA-N6-TCACA consensus defined in previous work (2, 16). Using the Virtual tool of the ProDoric database and the corresponding *E. coli* Crp position weight matrix, we scanned the 5'untranslated regions (UTR) of regulatory and structural genes of *B. cereus* F4430/73 enterotoxins. Figure 4A shows the locations of predicted Fnr binding boxes for *fnr*, *resDE*, *plcR*, *nhe*, *hbl1* and *hbl2* promoters and their positions relative to the transcriptional start point of each gene/operon. Except for *resDE* (Fig. 4B), the transcriptional start sites were identified in previous studies (1, 4). Three putative Fnr binding sites were found in the 5'UTR of the enterotoxin gene regulators *fnr*, *resDE* and *plcR*. Eight potential Fnr binding sites were found in the *nhe* promoter region: four were located upstream of the transcriptional start site, and four downstream. The *hbl* promoter region contained eleven potential Fnr binding sites, four located upstream of the +1 site and seven downstream.

To test whether apoFnr bound to the Fnr boxes predicted from the nucleotide sequence analysis, EMSAs were performed with both Fnr_{His} and Fnr_{His} and DNA fragments containing 5'UTR of *fnr*, *resDE*, *plcR*, *hbl* and *nhe*. In view of its size (1157 bp), the 5'UTR of *hbl* was first divided into two overlapping fragments of 636 pb (*hbl1*) and 610 pb (*hbl2*), respectively, as defined in Fig. 4A. Figure 5 shows the EMSA results for the six fragments. Fnr_{His} bound to all the regions tested, while no DNA-binding activity could be detected with Fnr_{His} . The specificity of the binding was evidenced from the disappearance of complexes in competition assays using 50-fold excess of homologous unlabelled promoter regions and by the absence of any competition when an unlabelled heterologous DNA was used (data not shown). EMSAs in the negative control (Fig. 5G) showed that a shift above 6 μM apoFnr should be considered as the result of non-specific binding. In addition, the behaviour of apoFnr markedly differed in the gel-shift titration assay depending on the promoter regions. ApoFnr bound to *fnr* and *resDE* promoter regions in an ordered fashion giving two retarded species (complex I and II) below 6 μM . In contrast, an increasing amount of apoFnr resulted in a gradual decrease in the mobility of the protein-DNA complexes for *plcR*, *hbl* and *nhe* promoter regions, which appeared to be stabilized at higher protein concentrations. This suggests that, as more protein was added, the protein complex bound to the DNA increased proportionally in size, with the added apoFnr being distributed evenly among all the complexes. The smearing of these species during EMSA also suggested that these high molecular complexes were not stable and dissociated during electrophoresis. The EMSA data also showed that the *plcR*, *hbl* and *nhe* 5'UTR were bound by apoFnr with a lower affinity ($K_D \leq 0.4 \mu\text{M}$) than the *resDE* and *fnr* promoter regions ($K_D = 3$ and $4.5 \mu\text{M}$, respectively).

To test whether the oligomeric state regulated the DNA-binding activity of both Fnr_{His} and Fnr_{His} , the effect of the reducing agent DTT (200 mM) on the binding of Fnr_{His} and the effect of the oxidizing agent diamide (1 mM) on the binding of Fnr_{His} to all promoter regions

were investigated. Adding reductant resulted in the generation of $_{\text{Strep}}\text{Fnr}$ -DNA complex patterns similar to those obtained with Fnr_{His} (Fig. 5). The effect of DTT was reversible, addition of diamide (1 mM) abolishing $_{\text{Strep}}\text{Fnr}$ binding (data not shown). Likewise, Fnr_{His} showed no DNA-binding activity in the presence of diamide (data not shown). Thus the oligomeric state of apoFnr was found to critically affect its binding activity. The data also indicate that apoFnr was able to bind the *fnr*, *resDE*, *plcR*, *hbl* and *nhe* 5'UTR regions only when present predominantly as a monomer.

Discussion

Our previous studies showed that aerobic enterotoxin expression was regulated by both the transcriptional regulator Fnr and oxygen availability (or redox state) under aerobiosis (4, 33). In the present work, we describe experimental evidence for redox regulation of enterotoxin gene expression mediated by Fnr through its DNA binding properties.

B. cereus apoFnr was overexpressed in *E. coli* and purified as either a C-terminal His-tagged (Fnr_{His}) or an N-terminal Strep-tagged ($_{\text{Strep}}\text{Fnr}$) fusion protein. Unlike Fnr_{His} , $_{\text{Strep}}\text{Fnr}$ was purified without affinity chromatography step. The reason was the poor affinity of Strep tag peptide for streptavidin (strepTactin) due to its fusion to the N-terminus of Fnr (19). No such problem was encountered in the case of Strep-tagged *B. subtilis* Fnr (27). This different behavior may be explained by the marked difference in the two N-terminal polypeptide sequences. Both recombinant Fnr (Fnr_{His} and $_{\text{Strep}}\text{Fnr}$) were produced in multiple oligomeric apoforms. The distribution of quaternary structures was shown to differ between the two tagged variants. Purified Fnr_{His} was predominantly monomeric, while $_{\text{Strep}}\text{Fnr}$ was predominantly oligomeric, the oligomerization of $_{\text{Strep}}\text{Fnr}$ appearing to be due to the formation of disulphide bridges. Data obtained from crystal structure analysis of a member of the Crp/Fnr family showed that dimerization involved the C-terminal domain (13). This

suggests that extension of *B. cereus* Fnr at its C-terminus may introduce steric hindrance that reduces flexibility and (or) affects interdomain communication. In turn, this would result in a less permissive, locked conformation, rendering the thiol group less exposed for pairing to form the disulphide bond.

Our results showed that the active DNA-binding form of both recombinant apoFnrs was the monomer. Diamide treatment inactivated monomeric apoFnr in a DTT-reversible manner, suggesting that it was subject to redox regulation. In addition, we detected the presence of disulfide-linked endogeneous dimers in *B. cereus* cells. Taken together, these findings suggest that formation of stabilized dimeric apoFnr by means of one or more SS bonds may be a regulatory mechanism that controls Fnr binding under exposure to oxidizing conditions. Figure 6 shows the scheme we propose for the reversible activation/inactivation of *B. cereus* apoFnr. It implies that this protein mediates a response to oxygen concentration and (or) redox state causing the repression or activation of relevant genes. Such a thiol-based redox switch has been observed with *Desulfitobacterium dehalogenans* CrpK, a member of the Crp/Fnr family (24, 25). In this bacterium, the redox switch involves formation of an intermolecular disulphide bond that links two CprK subunits in an inactive dimer. Although it belongs to the same family, *B. cereus* Fnr contains three more cysteines than CprK and should have the capacity to bind a FeS cluster like *B. subtilis* Fnr (27). For this reason, our findings are original. Additional work is now required to determine which of the seven cysteine residues are involved in this redox state sensing.

Many transcription factors bind DNA to form dimeric protein-DNA complexes. For these proteins, there are two limiting pathways that can describe the route of complex assembly. The protein can dimerize first, and then associate with DNA (dimer pathway), or can follow a pathway in which two monomers bind DNA sequentially and assemble their dimerization interface while bound to DNA (monomer pathway) (15). Many regulators bind

DNA by the dimer pathway, and this is the case for Fnr of *B. subtilis* and *E. coli* under anaerobiosis (27). Under aerobiosis, apoFnr is produced as an inactive monomer in *E. coli* (28) and as an inactive dimer in *B. subtilis* (27). Because only the monomeric form of *B. cereus* apoFnr binds to DNA, we propose that Fnr binding in *B. cereus* occurs via the monomer pathway under aerobiosis (Fig. 6). Binding through the monomer pathway allows a dimeric transcription factor to respond rapidly to stimuli and to locate its target site quickly without becoming entrapped kinetically at a non-specific site (23). Therefore, in addition to a faster assembly of apoFnr-DNA complexes in response to oxygen tension in the environment allowed by the monomer pathway, an efficient way to discriminate between specific and non-specific target sites is also provided.

Since apoFnr bound to the promoter regions of *fnr* itself, the two-component system *resDE*, the virulence regulator *plcR* and the enterotoxin genes *hbl* and *nhe*, we concluded that apoFnr directly controlled both its own expression and that of *resDE*, *plcR*, *hbl* and *nhe* (34). The relatively low DNA binding affinity observed for apoFnr suggests that other factors may be involved in DNA recognition as well as in protein-DNA complex stabilization (16). For example, it is conceivable that apoFnr operates with a specific oxidoreductase system or that for some other reason the cytoplasmic environment provided by *B. cereus* enhances its site-specific DNA binding ability. In addition, interaction of apoFnr with one or more other regulatory proteins may facilitate its interaction with DNA. High affinity binding to 5'UTR regions of enterotoxin genes may require apoFnr-PlcR interaction insofar as PlcR (1) possesses binding sites close to the predicted Fnr binding sites (Fig. 4A). Another possible interaction partner of apoFnr is the redox regulator ResD (4).

Transcriptional regulators such as members of the Crp/Fnr family interact with the α subunit of RNA polymerase (RNAP) (10). It has been shown that the protein-protein interaction increases the affinity of both partners to the promoter site (2). The contacts

438 established between a Crp/Fnr protein and RNAP involve three patches of surface-exposed
439 amino acids (called activating regions 1, 2, and 3) of Crp/Fnr protein. These contacts depend
440 on the specific architecture of each promoters. The Crp/Fnr -dependent promoters can be
441 grouped into three classes (labelled I, II, and III) based on the number and position of the
442 Crp/Fnr binding sites relative to the start of transcription, and on the mechanism for
443 transcription activation (2). The upstream DNA binding site in class I promoters is centred
444 either at position -61.5 (*i.e.*, its axis of symmetry is between positions -61 and -62) or one to
445 three helical turns further upstream (*i.e.*, -71.5 , -82.5 , or -92.5). In class II promoters, the
446 symmetry axis of the binding site is located at position -41.5 relative to the transcription start
447 site, thus overlapping with the -35 region. Class III promoters comprise two or more DNA-
448 binding sites for Crp/Fnr and have various architectures according to both the spacing
449 between the DNA binding sites and the distance between the Crp/Fnr and the RNAP-DNA
450 binding sites. In the case of *B. cereus*, the location of predicted Crp/Fnr binding sites
451 upstream of the transcriptional start site suggests that the *B. cereus fnr* promoter region is a
452 class I activating promoter, while *resDE* and *plcR* promoter regions are class II promoters.
453 The *nhe* and *hbl* promoters are different and may be considered as class III Crp/Fnr-dependent
454 activated promoters. However, *nhe*, *hbl*, and to a lesser extent *fnr*, *resDE* and *plcR* promoter
455 regions, also contain predicted Crp/Fnr boxes located close to the -10 region and (or)
456 downstream of the transcriptional start site *i.e* at positions different from those found in
457 classical Crp/Fnr activated promoters. Comparable results were found for *E. coli* and *B.*
458 *subtilis* Fnr (9, 27), where repression of transcription is mediated by Fnr binding to sites
459 differently located compared with activate sites. Thus we hypothesize that the regulation of
460 enterotoxin gene expression involves an interplay of transcriptional activation and repression
461 by Fnr. Repression may be mediated by occupancy of sites located downstream of the $+1$ site.
462 In conclusion, the mechanism of Fnr-dependent regulation of enterotoxin in *B. cereus* is

undoubtedly complex, and further extensive studies are required to examine the essential role of the downstream binding sites. Importantly, both *hbl* and *nhe* promoters have a long UTR (Fig. 4A), making it likely that mechanisms at the post-transcriptional level also control their expression. Such regulation could involve interaction between transcriptional regulator and ribosomal proteins (8). Finally, deciphering the complexities of this Fnr-dependent regulation is necessary to fully understand the mechanisms employed by *B. cereus* to ensure optimal virulence gene expression in response to changes in oxygen tension such as those encountered during infection in a human host.

In conclusion, this work shows that unlike its homolog in *B. subtilis* (12, 27), *B. cereus* Fnr is able to function as a transcriptional factor independently of the integrity of the FeS cluster. Thus *B. cereus* Fnr illustrates the great versatility of the archetypal Crp/Fnr structure for transducing environmental signals to the transcriptional apparatus. More importantly, this study expands our knowledge of the molecular mechanisms used in *B. cereus* to modulate the transcriptional level of enterotoxin genes in response to redox variations.

ACKNOWLEDGEMENTS

J.E. held a fellowship from the Ministère de la Recherche et de l'Enseignement supérieur. We thank Christine Meyer (CEA-Grenoble) for her help and technical advice in protein purification, Bernard Fernandez (CEA-Marcoule) for conducting DLS experiments, Jean-Charles Gaillard (CEA-Marcoule) for mass spectrometry measurements and Dr. Valérie Tanchou (CEA-Marcoule) for her kind help in the production of polyclonal antibodies.

REFERENCES

- 487 1. **Agaisse, H., M. Gominet, O. A. Okstad, A. B. Kolsto, and D. Lereclus.** 1999. PlcR
488 is a pleiotropic regulator of extracellular virulence factor gene expression in *Bacillus*
489 *thuringiensis*. Mol Microbiol **32**:1043-1053.
- 490 2. **Busby, S., and R. H. Ebright.** 1999. Transcription activation by catabolite activator
491 protein (CAP). J Mol Biol **293**:199-213.
- 492 3. **Duport, C., S. Thomassin, G. Bourel, and P. Schmitt.** 2004. Anaerobiosis and low
493 specific growth rates enhance hemolysin BL production by *Bacillus cereus* F4430/73.
494 Arch Microbiol **182**:90-95.
- 495 4. **Duport, C., A. Zigha, E. Rosenfeld, and P. Schmitt.** 2006. Control of enterotoxin
496 gene expression in *Bacillus cereus* F4430/73 involves the redox-sensitive ResDE
497 signal transduction system. J Bacteriol **188**:6640-6651.
- 498 5. **Folta-Stogniew, E.** 2006. Oligomeric states of proteins determined by size-exclusion
499 chromatography coupled with light scattering, absorbance, and refractive index
500 detectors. Methods Mol Biol **328**:97-112.
- 501 6. **Gabant, G., J. Augier, and J. Armengaud.** 2007. Assessment of solvent residues
502 accessibility using three Sulfo-NHS-biotin reagents in parallel: application to footprint
503 changes of a methyltransferase upon binding its substrate. J Mass Spectrom **43**:360-
504 370
- 505 7. **Gohar, M., O. A. Okstad, N. Gilois, V. Sanchis, A. B. Kolsto, and D. Lereclus.**
506 2002. Two-dimensional electrophoresis analysis of the extracellular proteome of
507 *Bacillus cereus* reveals the importance of the PlcR regulon. Proteomics **2**:784-791.
- 508 8. **Gray, J. P., J. W. Davis, 2nd, L. Gopinathan, T. L. Leas, C. A. Nugent, and J. P.**
509 **Vanden Heuvel.** 2006. The ribosomal protein rpL11 associates with and inhibits the
510 transcriptional activity of peroxisome proliferator-activated receptor-alpha. Toxicol
511 Sci **89**:535-546.

9. **Green, J., A. S. Irvine, W. Meng, and J. R. Guest.** 1996. FNR-DNA interactions at natural and semi-synthetic promoters. *Mol Microbiol* **19**:125-137.
10. **Green, J., C. Scott, and J. R. Guest.** 2001. Functional versatility in the CRP-FNR superfamily of transcription factors: FNR and FLP. *Adv Microb Physiol* **44**:1-34.
11. **Guinebretiere, M. H., and C. Nguyen-The.** 2003. Sources of *Bacillus cereus* contamination in a pasteurized zucchini purée processing line, differentiated by two PCR-based methods. *FEMS Microbiol Ecology* **43**:207-215.
12. **Guinebretiere, M. H., F. L. Thompson, A. Sorokin, P. Normand, P. Dawyndt, M. Ehling-Schulz, B. Svensson, V. Sanchis, C. Nguyen-The, M. Heyndrickx, and P. De Vos.** 2007. Ecological diversification in the *Bacillus cereus* Group. *Environ Microbiol* **10**:851-865.
13. **Joyce, M. G., C. Levy, K. Gabor, S. M. Pop, B. D. Biehl, T. I. Doukov, J. M. Ryter, H. Mazon, H. Smidt, R. H. van den Heuvel, S. W. Ragsdale, J. van der Oost, and D. Leys.** 2006. CprK crystal structures reveal mechanism for transcriptional control of halorespiration. *J Biol Chem* **281**:28318-28325.
14. **Khoroshilova, N., H. Beinert, and P. J. Kiley.** 1995. Association of a polynuclear iron-sulfur center with a mutant FNR protein enhances DNA binding. *Proc Natl Acad Sci U S A* **92**:2499-2503.
15. **Kohler, J. J., S. J. Metallo, T. L. Schneider, and A. Schepartz.** 1999. DNA specificity enhanced by sequential binding of protein monomers. *Proc Natl Acad Sci U S A* **96**:11735-11739.
16. **Korner, H., H. J. Sofia, and W. G. Zumft.** 2003. Phylogeny of the bacterial superfamily of Crp-Fnr transcription regulators: exploiting the metabolic spectrum by controlling alternative gene programs. *FEMS Microbiol Rev* **27**:559-592.

- 536 17. **Kotiranta, A., K. Lounatmaa, and M. Haapasalo.** 2000. Epidemiology and
537 pathogenesis of *Bacillus cereus* infections. *Microbes Infect* **2**:189-198.
- 538 18. **Laemmli, U. K.** 1970. Cleavage of structural proteins during the assembly of the head
539 of bacteriophage T4. *Nature* **227**:680-685.
- 540 19. **Maier, T., N. Drapal, M. Thanbichler, and A. Bock.** 1998. Strep-tag II affinity
541 purification: an approach to study intermediates of metalloenzyme biosynthesis. *Anal*
542 *Biochem* **259**:68-73.
- 543 20. **Okstad, O. A., M. Gominet, B. Purnelle, M. Rose, D. Lereclus, and A. B. Kolsto.**
544 1999. Sequence analysis of three *Bacillus cereus* loci carrying PlcR-regulated genes
545 encoding degradative enzymes and enterotoxin. *Microbiology* **145**:3129-3138.
- 546 21. **Ouhib, O., T. Clavel, and P. Schmitt.** 2006. The Production of *Bacillus cereus*
547 Enterotoxins Is Influenced by Carbohydrate and Growth Rate. *Curr Microbiol* **53**:222-
548 226.
- 549 22. **Pelley, J. W., C. W. Garner, and G. H. Little.** 1978. A simple rapid biuret method
550 for the estimation of protein in samples containing thiols. *Anal Biochem* **86**:341-3.
- 551 23. **Pomerantz, J. L., S. A. Wolfe, and C. O. Pabo.** 1998. Structure-based design of a
552 dimeric zinc finger protein. *Biochemistry* **37**:965-970.
- 553 24. **Pop, S. M., N. Gupta, A. S. Raza, and S. W. Ragsdale.** 2006. Transcriptional
554 activation of dehalorespiration. Identification of redox-active cysteines regulating
555 dimerization and DNA binding. *J Biol Chem* **281**:26382-26390.
- 556 25. **Pop, S. M., R. J. Kolarik, and S. W. Ragsdale.** 2004. Regulation of anaerobic
557 dehalorespiration by the transcriptional activator CprK. *J Biol Chem* **279**:49910-8.
- 558 26. **Ramarao, N., and D. Lereclus.** 2006. Adhesion and cytotoxicity of *Bacillus cereus*
559 and *Bacillus thuringiensis* to epithelial cells are FlhA and PlcR dependent,
560 respectively. *Microbes Infect* **8**:1483-91.

27. **Reents, H., I. Gruner, U. Harmening, L. H. Bottger, G. Layer, P. Heathcote, A. X. Trautwein, D. Jahn, and E. Hartig.** 2006. *Bacillus subtilis* Fnr senses oxygen via a [4Fe-4S] cluster coordinated by three cysteine residues without change in the oligomeric state. *Mol Microbiol* **60**:1432-1445.
28. **Reinhart, F., S. Achebach, T. Koch, and G. Unden.** 2007. Reduced ApoFNR as the major form of FNR in aerobically growing *Escherichia coli*. *J Bacteriol* **190**:879-886.
29. **Rosenfeld, E., C. Duport, A. Zigha, and P. Schmitt.** 2005. Characterisation of aerobic and anaerobic vegetative growth of the food-borne pathogen *Bacillus cereus*. *J Can Microbiol* **51**:149-158.
30. **Schoeni, J. L., and A. C. Wong.** 2005. *Bacillus cereus* food poisoning and its toxins. *J Food Prot.* **68**:636-648.
31. **Slamti, L., and D. Lereclus.** 2002. A cell-cell signaling peptide activates the PlcR virulence regulon in bacteria of the *Bacillus cereus* group. *Embo J* **21**:4550-4559.
32. **Spira, W. M., and J. M. Goepfert.** 1975. Biological characteristics of an enterotoxin produced by *Bacillus cereus*. *Can J Microbiol* **21**:1236-1246.
33. **Zigha, A., E. Rosenfeld, P. Schmitt, and C. Duport.** 2006. Anaerobic cells of *Bacillus cereus* F4430/73 respond to low oxidoreduction potential by metabolic readjustments and activation of enterotoxin expression. *Arch Microbiol* **185**:222-233.
34. **Zigha, A., E. Rosenfeld, P. Schmitt, and C. Duport.** 2007. The redox regulator Fnr is required for fermentative growth and enterotoxin synthesis in *Bacillus cereus* F4430/73. *J Bacteriol* **189**:2813-2824.

FIGURE LEGEND

Figure 1: Gel filtration and DLS chromatograms of purified Fnr proteins. Fnr_{His} (Panel A), Fnr_{Strep} (Panel B) and reduced Fnr_{Strep} (Panel C) were injected (~300 µg in 100 µl) into a Superdex 200 column (HR 10/30) with TRIS-HCl 50 mM (pH 8.3), NaCl 120 mM as eluant at a flow rate of 0.5 ml/min. DTT (10 mM) was added to the elution buffer to determine the oligomeric state of reduced Fnr_{Strep} (Panel C). The black and grey lines correspond to the light scattering (LS) signal and the UV signal recorded at 280 nm, respectively. These signals were normalized as 0-1 ratio for comparison (left axis). The molecular weight estimates of the major peaks are also indicated in dashed lines (right axis).

Figure 2: SDS-PAGE analysis of the oligomeric nature of _{Strep}Fnr and Fnr_{His}. Panels A and B: effect of DTT on _{Strep}Fnr (Panel A) and Fnr_{His} (Panel B) oligomerization. Purified proteins were incubated with 0, 10, 50, 100 or 200 mM DTT (lanes 2-6, respectively). Recombinant proteins were then subjected to non-reducing SDS-PAGE. The arrows indicate monomers (m), dimers (d) and higher oligomers (o). Standard proteins (Lane 1) are shown. Panel C SDS-PAGE profile of Fnr_{His} cross-linked with EDC. Fnr_{His} (5 µM) was cross-linked with EDC. Products were visualized by immunoblotting with anti-His antibody. Lane 1, cross-linked Fnr_{His}. Lane 2, untreated Fnr_{His}. Panel D: Non-denaturing SDS-PAGE profile of Fnr_{His} cross-linked with diamide. Lane 1, standard proteins. Lane 2, untreated Fnr_{His}; Lanes 3 & 4, disulphide linked Fnr_{His} with 1 mM and 10 mM diamide, respectively. The arrows indicate monomers (m), dimers (d), trimers (t) and higher oligomers (o).

Figure 3: Western blot detection of endogeneous Fnr species from *B. cereus* cells. Lysates of *B. cereus* F4430/73 wild-type (wt) and *fnr* mutant were probed with polyclonal Fnr

antiserum. Both strains were grown in regulated batch culture (pH 7.2) under aerobiosis (4). Proteins were separated by non-reducing SDS-PAGE. Lane: 1, Fnr_{Strep} purified from *E. coli*. Lane 2, *fnr* mutant. Lane 3, Wild-type strain. Putative identities shown on the right were determined for the wild-type strain on the basis of results obtained with both recombinant Fnr and *fnr* mutant strains. The arrows indicate monomer (m) and dimer (d) forms. The position and mass (kDa) of molecular weight marker are given in the left.

Figure 4: Potential Fnr binding sites in the 5' untranslated regions of *fnr*, *resDE*, *plcR*, *hbl*, and *nhe*. All numbering is relative to the transcription start site at position +1. Panel A: potential Fnr binding sites are shown relative to the transcription start site as grey boxes. PlcR boxes are highlighted by dark boxes. Panel B: genetic organization of the *resDE* promoter region. The transcriptional start site (+1) determined by 5'-RACE PCR is in bold. The putative -35 and -10 motifs are underlined. Putative Crp/Fnr boxes are indicated by a grey background.

Figure 5: Binding of apoFnr to 5'UTR regions of *fnr*, *resDE*, *plcR*, *hbl*, and *nhe* genes determined by EMSA. DNA corresponding to *fnr* (A), *resDE* (B), *plcR* (C), *hbl1* (D), *hbl2* (E), *nhe* (F) and a negative control (G) were bound with increasing concentrations of apoFnr as indicated. The results presented are representative examples of an experiment performed in triplicate with either purified Fnr_{His} or with reduced _{Strep}Fnr (purified _{Strep}Fnr + 200 mM DTT). Lanes 1 to 10: 0, 0.2, 0.4, 0.6, 0.8, 1, 2, 3, 4, 5, and 6 μ M of protein, respectively.

Figure 6: Proposal for the regulation of apoFnr activity by a thiol-disulphide redox switch. Brackets indicate that one or more disulphide bonds may be involved.

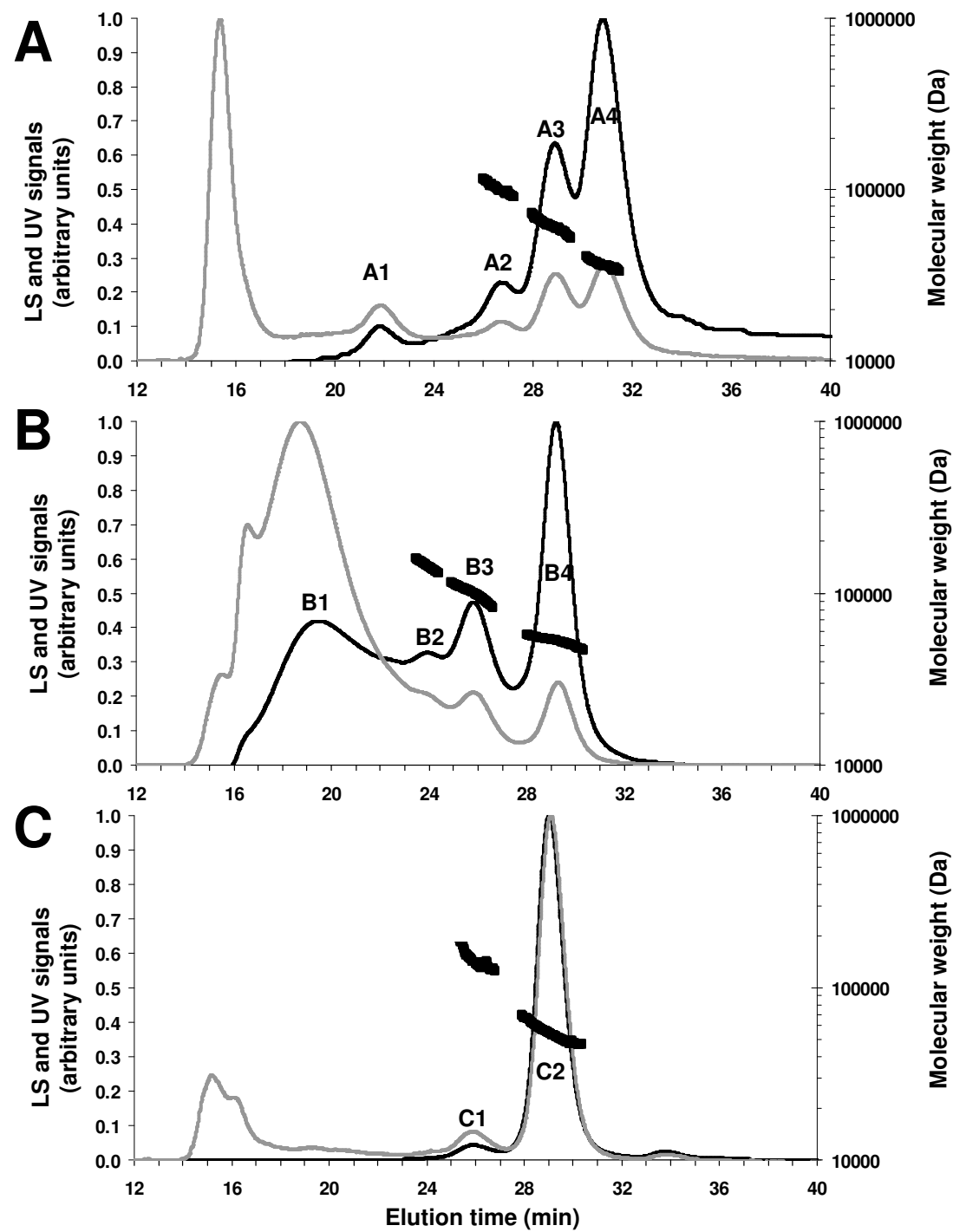


Figure 1

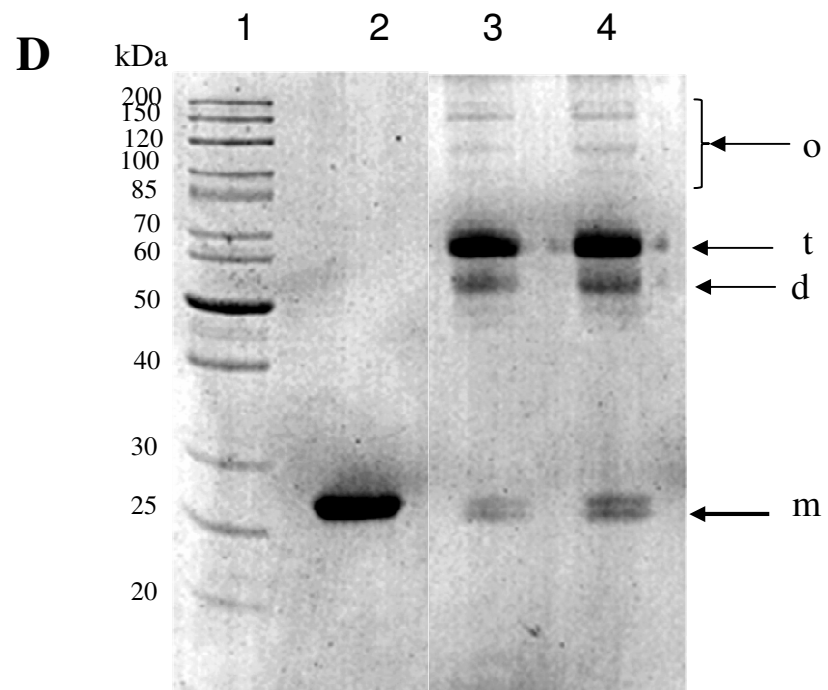
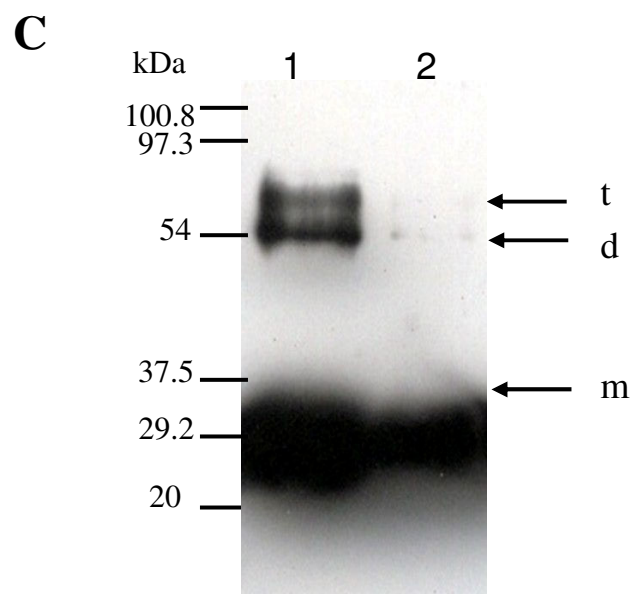
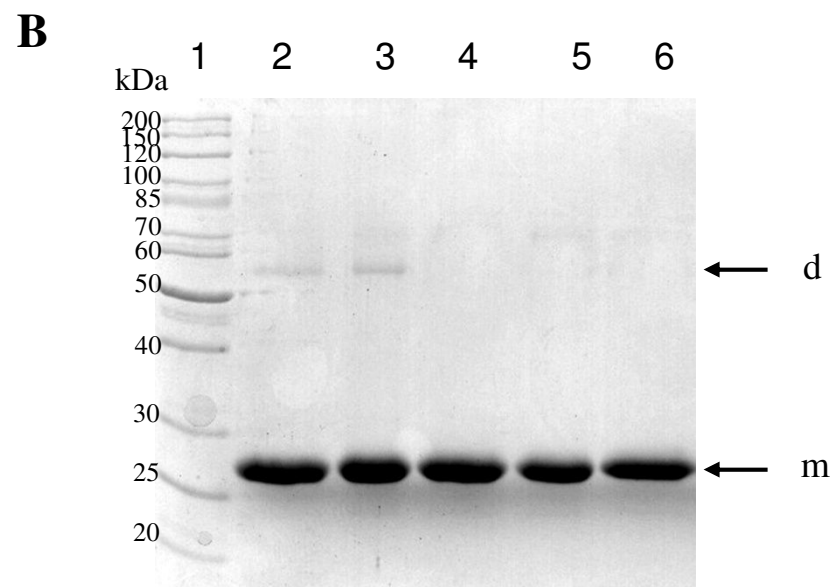
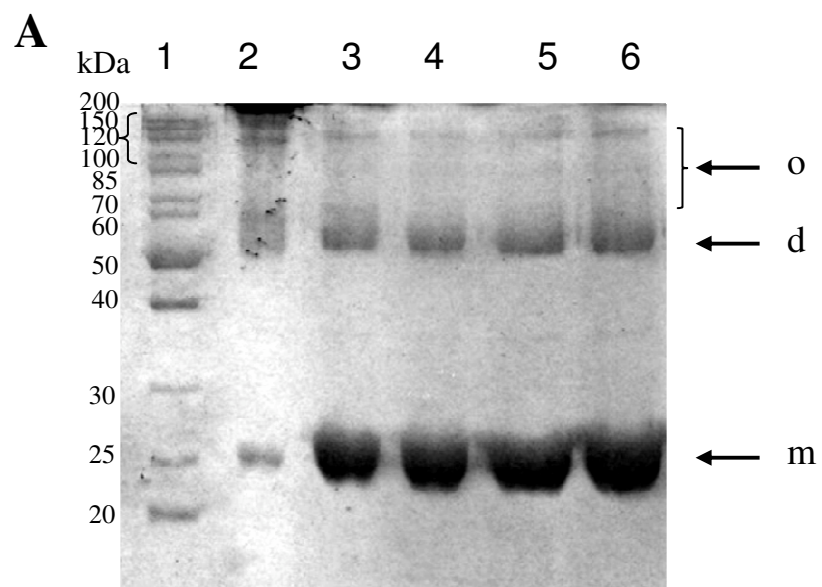


Figure 2

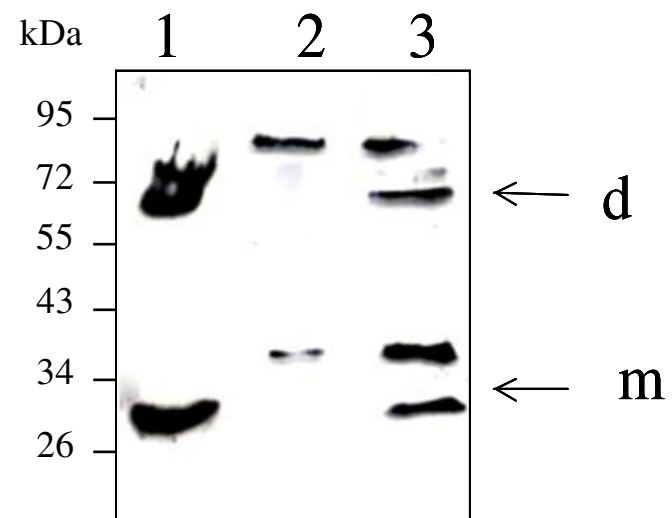
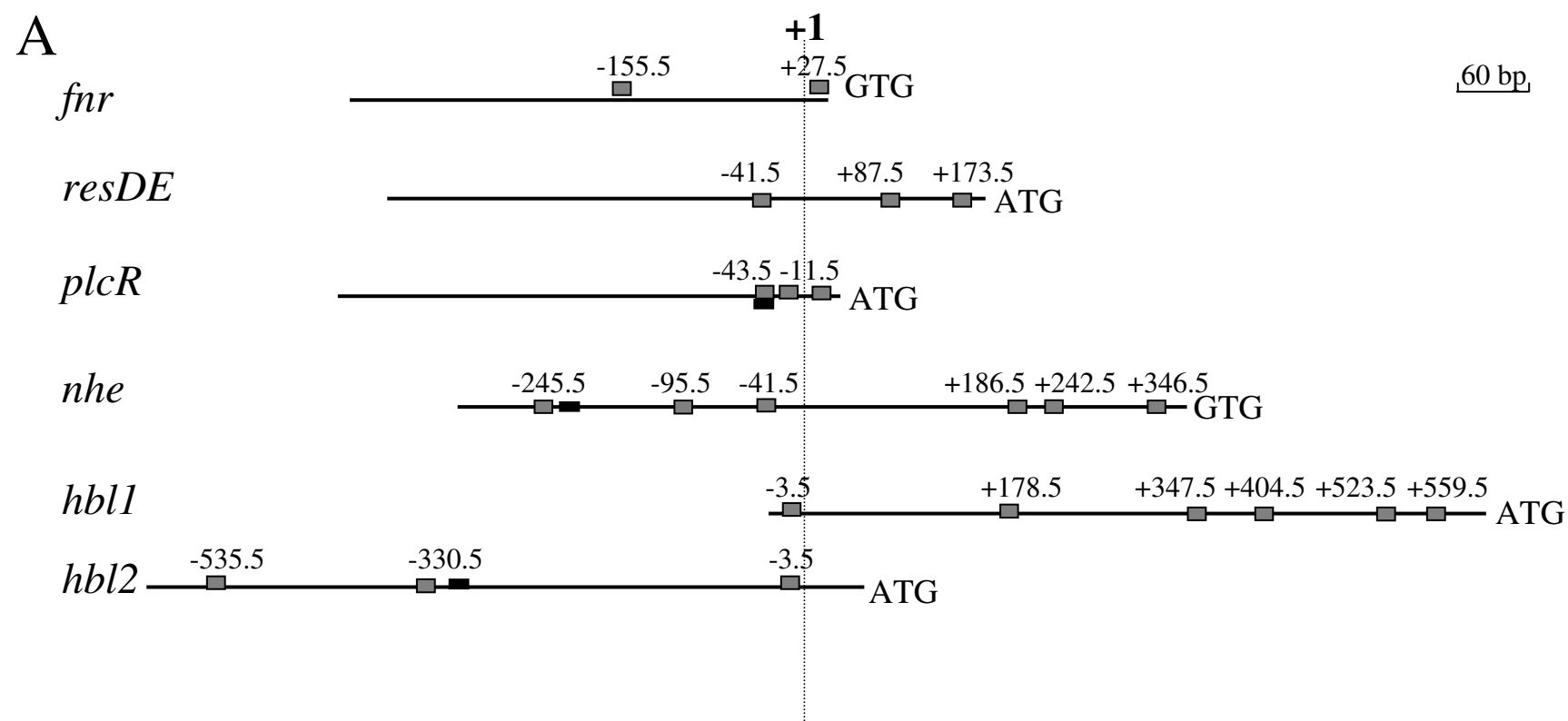


Figure 3



B

-62 TTTTCTTCTTT TTTGAGAAAAACATGACA AAGTAGCGGTTGATTTTGTA AAATGATGTCGAGGACATTATATGCT +13

GTTCAAAAAAATACATAGTTTTGGAAAAAATTGAACAAAATTTATTATTCTTGTGAAGCATGATATGGGAAGT +88

GAAACATTTAGAAGATTGCTTAAATAAACGAGAATAGCGCAACATAATAGTTAAAGAAGGGTAGGTGTGAACCGC +163

TGAGGTGAGAGTGCGCAGCGGGTAGAGATG +193

Figure 4

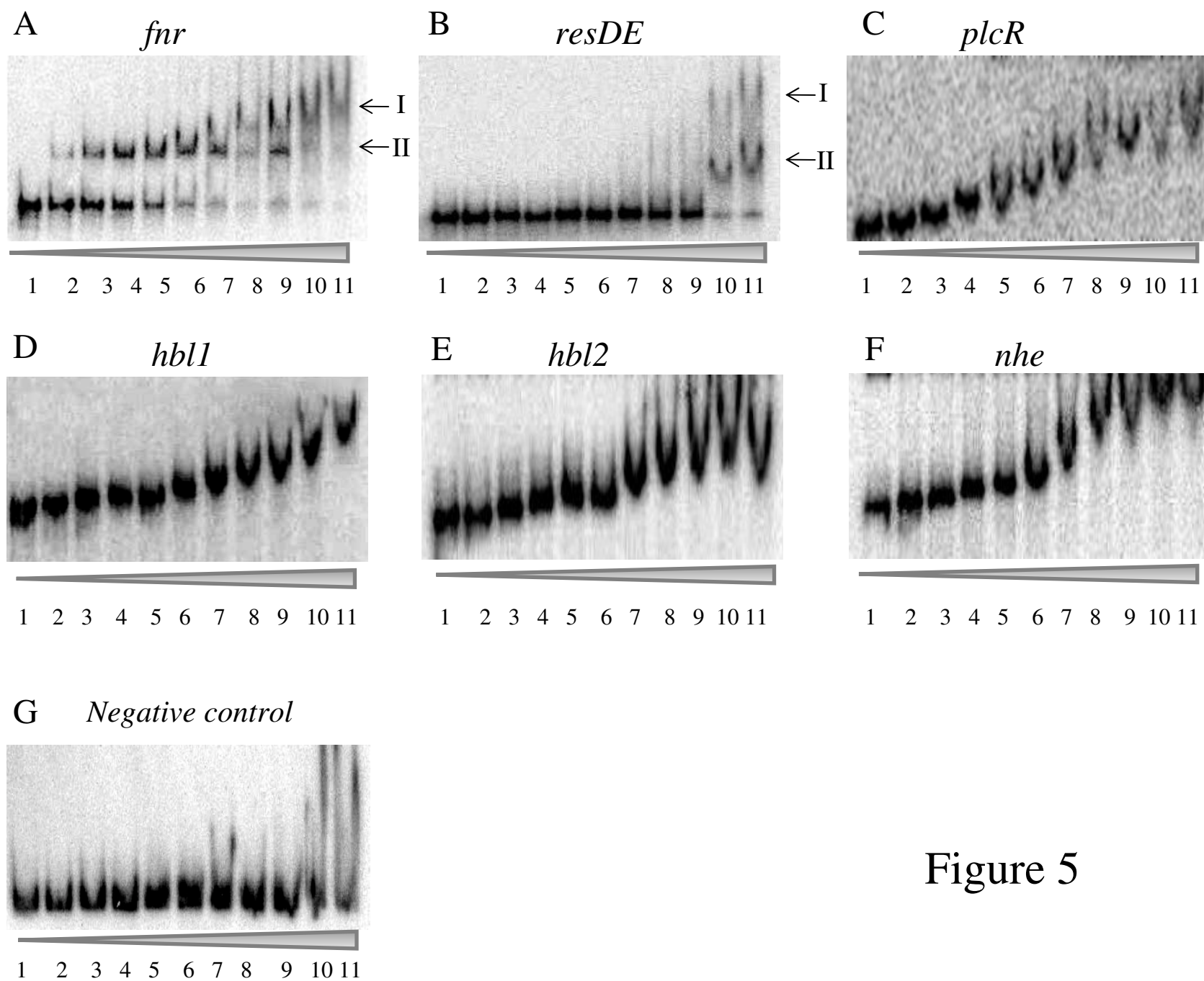


Figure 5

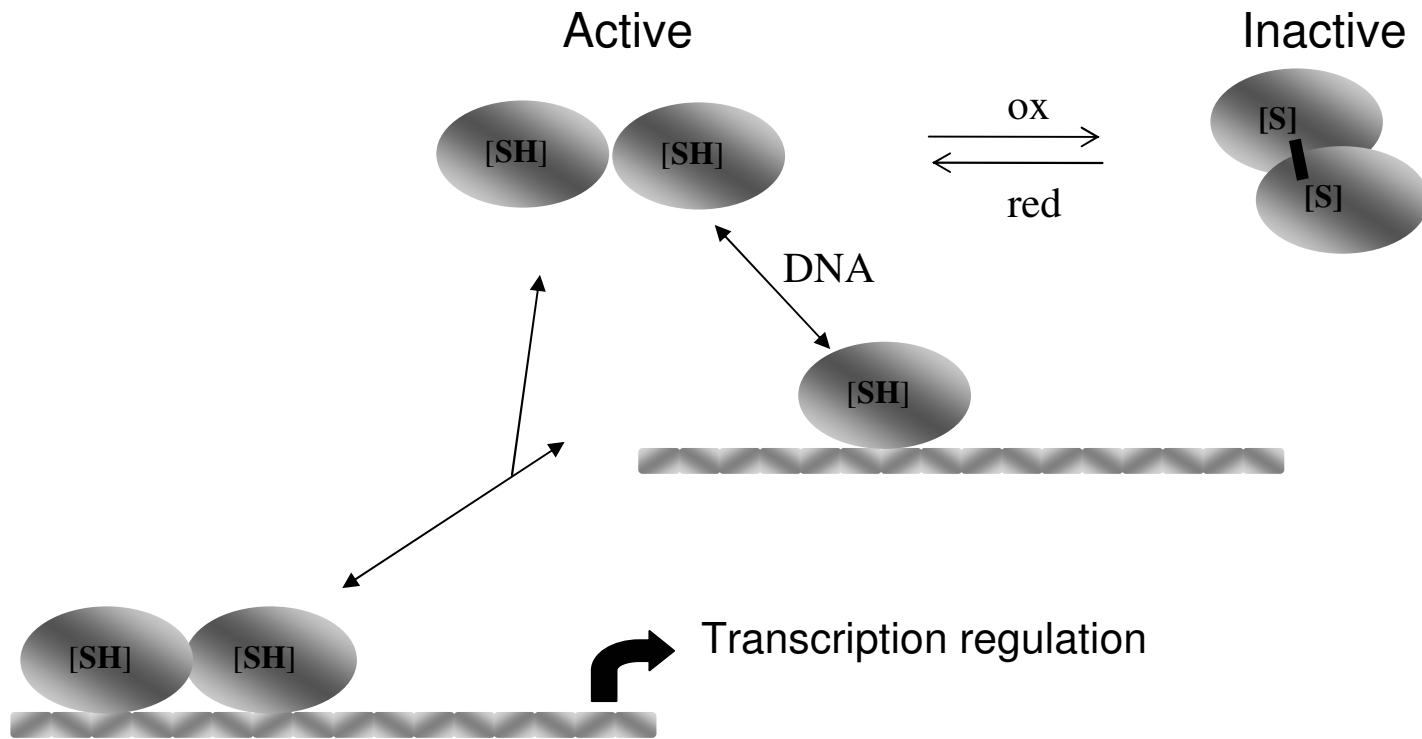


Figure 6